


 CrossMark
 click for updates

Cite this: RSC Adv., 2016, 6, 42701

 Received 19th February 2016
 Accepted 21st April 2016

DOI: 10.1039/c6ra04480h

www.rsc.org/advances

One-stage synthesis of $\text{FcP(O)(OC}_2\text{H}_5)_2$ from ferrocene and α -hydroxyethylphosphonate

Mikhail Khrizanforov, Sofia Strekalova, Kirill Kholin, Vera Khrizanforova, Valeriya Grinenko, Tatyana Gryaznova and Yulia Budnikova*

A new approach is proposed for ferrocene phosphorylation using α -hydroxylalkylphosphonate as a "masked" phosphorylating agent, by electrochemical reduction of a ferrocene and $(\text{Me})_2\text{C(OH)P(O)(OC}_2\text{H}_5)_2$ mixture at -50 °C. The method makes it possible to obtain the product of diethyl ferrocenyl phosphonate with a high yield (87–89%) and 100% conversion of the initial phosphonate in one stage. It is evidenced with experiments that ferrocene reduction is carried out with preservation of the iron charge in the ferrocene fragment and with the formation of a cyclopentadienyl ligand radical anion at -3.3 V ref. Ag/AgCl (at -50 °C).

Introduction

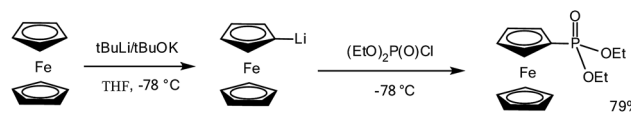
Ferrocene derivatives with phosphorus-containing substituents (phosphines, phosphonic acid moieties, *etc.*) gave rise to a new class of organophosphorus compounds, which are very powerful ligands that have unique features in metal-catalyzed organic reactions.^{1–15}

Ferrocene-bearing ligands proved to be prospective precursors in the design of various complexes and coordination polymers, which possess interesting and practically applicable physical features. The electrochemical, magnetic, luminescent and nonlinear optical features of coordination polymers with ferrocene fragments are of particular significance.^{3,7,16–20} This is due to the specific geometries that the ferrocenyl moiety can determine as well as to its electronic (redox) properties. Ferrocene can be regarded as a universal modifier for organic compounds and biomolecules. Due to stable sandwich structure and reversibility of oxidation under physiological pH, ferrocene can be used as a redox-active but nonradioactive label.^{21–24} Moreover, with its high lipophilicity, ferrocene easily penetrates cell and nuclear membranes and overcomes the blood brain barrier. Ferrocene as a carrier (or, in modern terms, a vector) can be used for the delivery of other molecules through membranes. It is important that the toxicity of organic compounds decreases upon Fc modification.^{24,25} Ferrocenyl organophosphorus ligands are usually stable, easy to handle and often isolable as optical stereoisomers. Ferrocenyl phosphine ligands are able to form complexes with transition metals in a variety of coordinative geometries and oxidation states,

thus producing efficient catalyst precursors for many chemical transformations.^{1,16}

The first attempts to introduce a phosphorous substituent to a ferrocene by means of $(\text{EtO})_2\text{P(O)H}$ free-radical phosphorylation occurred as early as 1962;²⁶ however, they were unsuccessful. It was shown that mixing a ferrocene suspension in phosphorous trichloride PCl_3 with aluminum chloride AlCl_3 and a subsequent hydrolysis of the reaction mixture would lead to the formation of ferrocenyl(*H*-phosphinic)acid and 1,1'-ferrocenyl-bis(*H*-phosphinic)acid with a low yield of 3–5%.²⁷ The use of (dimethylamine)dichlorophosphine $\text{Me}_2\text{NPtCl}_2$ as the phosphorylating reagent somehow made it possible to increase the yield of the acid to 9%.²⁸ Ferrocenyl(phenyl)phosphonic acid was obtained with a high yield of 92% in the course of the reaction of ethyl ether of ferrocenyl(phenyl)phosphonic acid $\text{Fc}(\text{Ph})\text{P(O)OEt}$ with Me_3SiBr and subsequent hydrolysis.²⁹ However, $\text{Fc}(\text{Ph})\text{P(O)OEt}$ obtaining is based on the use of a hazardous gas Cl_2 , which makes this method much less attractive.

The most frequent method of synthesis of ferrocene derivatives with phosphorus-containing substituents is based on the metallation of ferrocene (for instance, with butyllithium) or its derivatives with a subsequent addition of chlorophosphine electrophile.^{16,18,29–33} Diethyl ferrocenyl phosphonate FcP(O)(OEt)_2 was obtained with the yield of 33% using a reaction of ferrocene monolithium with diethylchlorophosphate $(\text{EtO})_2\text{P(O)Cl}$ at 0 °C.²⁷



Scheme 1 Multi-stage approach to the synthesis of ferrocene derivatives.



The addition of a base *t*BuOK facilitated an increase in yield to 79% (at -78°C in THF, Scheme 1).³²

This approach is multi-stage, as it includes the use of *t*-BuLi (after adding *tert*-butoxide to ferrocene) at a very low temperature -78°C at the first stage, and the use of a chlorinated derivative, *i.e.*, diethyl chlorophosphosphate, which is toxic, unstable and results in chlorine-containing byproducts, at the second stage.³² It is also disadvantageous to use the explosive solvent THF. For that reason, such a method is expensive and environmentally unacceptable.

The latest achievements in the field of direct phosphorylation of the $\text{C}(\text{sp}^2)\text{-H}$ bonds in a variety of aromatic substrates, including electrochemical functionalization, do not concern the phosphorylation of ferrocenes.³⁴⁻³⁷

Taking into account the importance of ferrocene derivatives with phosphor-containing substituents, search of new, more convenient, one-stage and selective approaches to their synthesis remains a relevant objective. The purpose of this work is to develop a method for the direct phosphorylation of ferrocene with α -hydroxylethylphosphonate under electrochemical reduction conditions and to identify the intermediate of this reaction.

Results and discussion

Electrochemical synthesis

A joint electrolysis of ferrocene and the phosphorylating agent α -hydroxylethylphosphonate $(\text{Me})_2\text{C}(\text{OH})\text{P}(\text{O})(\text{OC}_2\text{H}_5)_2$ at -50°C on a platinum electrode led to the formation of mono-substituted **1** (as the basic product) and disubstituted **2** diethyl ferrocenyl phosphonates $\text{FcP}(\text{O})(\text{OEt})_2$ with good yields (Table 1). The electrolysis potential was -3.3 V (ref. to Ag/AgCl), and alkali were used as basic additives to activate the “masked” phosphorylating reagent.

The use of Et_4NOH provides higher yield compared to NaOH , probably because, in the latter case, due to side reactions of sodium reduction and the formation of sparingly soluble sodium salts of phosphorous acids. Alkaline conditions are

necessary for a slow transformation of the “masked” phosphorylating agent into *H*-phosphonate by a known reaction,³⁸⁻⁴¹ which we assumed would be quickly captured by the reduced form of ferrocene. In the absence of Et_4NOH (or NaOH), phosphorylation with $(\text{CH}_3)_2\text{C}(\text{OH})\text{P}(\text{O})(\text{OEt}_2)$ does not occur.

Interestingly, in the proposed low-temperature conditions, phosphorous acid H_3PO_3 can also serve as a phosphorylating reagent using a lead cathode because it is not reduced in the available range of potentials on Pb at -50°C (Table 1, line 5, product **3**). An alkali activator is not required in this case. It should be noted that the lead cathode at low temperatures and high cathode potentials is gradually degraded, hence its use is limited to (by) only several cycles of synthesis. In this regard, preference was given to a platinum electrode and correspondingly suitable for it phosphorylated substrate, $(\text{Me})_2\text{C}(\text{OH})\text{P}(\text{O})(\text{OC}_2\text{H}_5)_2$. After passing of 1F of electricity (not 2F, as shown in Table 1), the yield reduced by *ca.* 10–12%. Further increase ($>2\text{F}$) of the passed current led to a decrease in yield and an unidentified byproducts formation. Ferrocene phosphorylation reaction with the use of dialkyl-*H*-phosphonate at the lead cathode occurs non-selectively, the yield of target product, determined by ^{31}P NMR spectra, was 35% (Table 1, line 4). Unidentified phosphorus-containing products were formed and the electrode was partially destroyed.

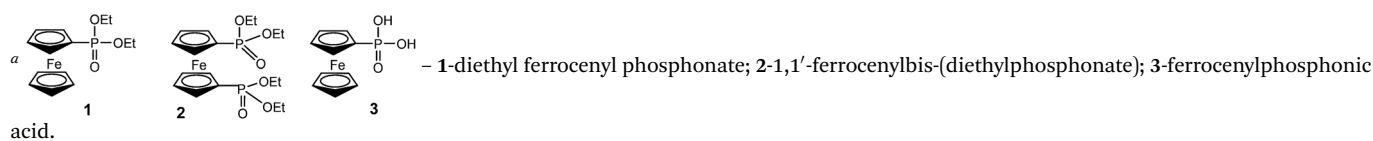
Voltammetry

Ferrocene and ferrocenyl derivatives are well known due to their ability to undergo a reversible one-electron oxidation,^{3,42} and the potential of Fc^+/Fc is the internal standard for electrochemical measurement,⁴³ the values of which have been measured in various aprotic and protonic solvents as well as in ionic liquids. Curiously, the reduction of ferrocene was studied in less detail, in single works that refer only to the voltammetry method.⁴⁴⁻⁴⁶

A high-purity solvent and electrochemical measurements at temperatures ranging from -45°C to -30°C have made it possible to observe a reversible one-electron reduction of ferrocene on mercury, platinum and glassy-carbon electrodes in DMF and dimethoxyethane.⁴⁵⁻⁴⁷ However, the voltammograms

Table 1 Reaction products of ferrocene phosphorylation, 2F electricity is passed, $T = -50^{\circ}\text{C}$, DMF as the solvent. Potentials from Ag/AgCl ref. electrode

No	Reagents and ratios	Base additive	Electrode/reaction potential	Product ^a yield
1	$\text{Fc} : (\text{CH}_3)_2\text{C}(\text{OH})\text{P}(\text{O})(\text{OEt})_2 [1 : 1]$	Et_4NOH	Pt/–3.3 V	1, 88% 2, 2%
2	$\text{Fc} : (\text{CH}_3)_2\text{C}(\text{OH})\text{P}(\text{O})(\text{OEt})_2 [1 : 2]$	Et_4NOH	Pt/–3.3 V	1, 60% 2, 12%
3	$\text{Fc} : (\text{CH}_3)_2\text{C}(\text{OH})\text{P}(\text{O})(\text{OEt})_2 [1 : 1]$	$\text{NaOH} + \text{Et}_4\text{NBF}_4$	Pt/–2.9 V	1, 61% 2, 6%
4	$\text{Fc} : \text{HP}(\text{O})(\text{OEt})_2 [1 : 1]$	Et_4NBF_4	Pb/–3.2 V	1, 35%
5	$\text{Fc} : \text{H}_3\text{PO}_3 [1 : 1]$	Et_4NBF_4	Pb/–3.3 V	3, 36%



are poorly reproducible, the approximate half-wave potential is -2.9 V (ref. electrode was not specified) at -37 °C (ref. 43) or -3.0 V at -90 °C in THF (ref. SCE).⁴⁵ It was assumed that, as a result of the reduction, a relatively unstable Cp_2Fe^- anion would be formed.⁴⁸ An increase in temperature leads to a two-electron reduction of the ferrocene and its decomposition, thereby forming metal iron on the mercury cathode.⁴⁶ Attempts were made to reduce the ferrocene in the CO atmosphere, and the formation of $[\text{CpFe}(\text{CO})_2]_2$ was observed.⁴⁹

We have assumed the reversibility of the ferrocene reduction at low temperatures and, accordingly, the relative stability of the reduced form (at least, in the time scale of the voltammetry) could be used to perform the functionalization-phosphorylation with its participation. The choice of partner for the coupling the ferrocene is limited by its reduction potential; that is, its E_p should be more negative than that of the ferrocene, or it should be electrochemically inactive in the accessible cathode range of the potentials. The voltammograms of investigated phosphorylating agents reduction on electrodes with low and high hydrogen overvoltage (Pt and Pd, correspondingly) at 25 °C and -50 °C, respectively, are shown in Fig. 1. Earlier it was known that dialkyl phosphites were reduced on electrodes with low hydrogen overvoltage at room temperature on platinum or glassy-carbon type electrodes in aprotic solvent in the presence of ammonium salts as supporting electrolyte,^{50,51} although in the range of high potentials, but still comparable with that for ferrocene. We can clearly see that voltammograms of phosphorus compounds with P–H bonds ($(\text{EtO})_2\text{PHO}$, H_3PO_3) have no pronounced reduction peaks on platinum, as noted previously,⁵¹ but their electrochemical activity is reflected in the sharp decrease of the limiting potential at which current increases, apparently due to the discharge of phosphoric acids and background electrolyte. The evolution of hydrogen, which can be observed visually, leads to oscillations in the voltammograms. The use of a lead electrode with high hydrogen overvoltage allows to extend the available range of potentials, because no electrode reaction up to -3.4 V is observed (Fig. 1).

Consequently, α -hydroxyethylphosphonate, so-called “masked” phosphorylating agent,^{38–41} is a more appropriate phosphorylating agent in our case (Table 1, lines 1–3). It is not reduced in the investigated accessible potential window in DMF on platinum cathode (Fig. 1) but is capable of slowly generating diethylphosphonate in the reaction mixture in the presence of a base.^{38–41}

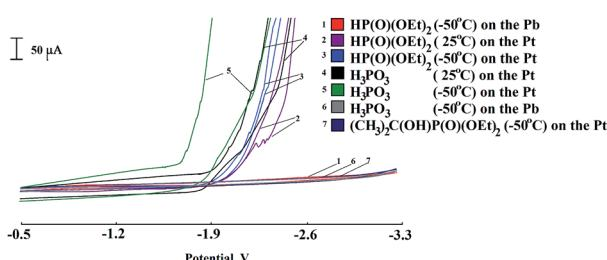


Fig. 1 Cyclic voltammograms of phosphorylating agents. Conditions: $T = 25$ and -50 °C, working electrodes Pt (2 mm^2) or Pb (16 mm^2), Ag/AgCl ref. electrode, 50 mM concentration, Bu_4NBF_4 , DMF, 100 mV s^{-1} .

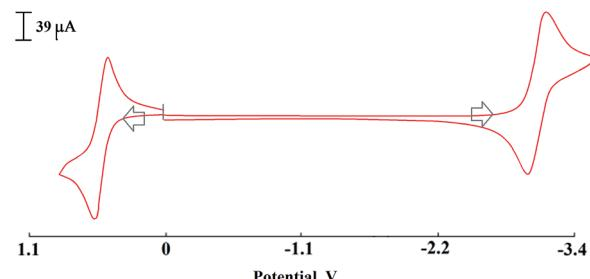


Fig. 2 Cyclic voltammogram of ferrocene. Conditions: $T = -50$ °C, glassy carbon working electrode, Ag/AgCl ref. electrode, 0.5 mM concentration, Bu_4NBF_4 , DMF, 100 mV s^{-1} .

Table 2 Ferrocene electrochemical features. Conditions: -50 °C, glassy carbon working electrode, Ag/AgCl ref. electrode, 0.5 mM [Fc], Bu_4NBF_4 background salt, DMF, 100 mV s^{-1}

Oxidation, Fc^0/Fc^+			Reduction, $\text{Fc}^0/\text{Fc}^{\bullet-}$		
$E_p^a/E_p^c, \text{V}$	$\Delta E_p^{\text{a-c}}, \text{V}$	$E_{1/2}, \text{V}$	$E_p^c/E_p^a, \text{V}$	$\Delta E_p^{\text{c-a}}, \text{V}$	$E_{1/2}, \text{V}$
0.62/0.53	0.09	0.57	-3.19/-3.01	0.18	-3.10

Cyclic voltammetry of ferrocene at the temperature of -50 °C is presented in Fig. 2 and Table 2. Accessible potential range increases at low temperatures. In the research conditions, two quasi-reversible peaks of oxidation and reduction of the ferrocene are observed, respectively. The quasi-reversible reduction at the potential of $E_{1/2} = -3.10$ V is well matched to the results of the ESR experiments, evidencing the formation of stable radical anions at this potential. The addition of a single electron to a neutral (uncharged) molecule generates chemical species called the radical anion (in our case, ferrocene radical-anion),⁵² which simultaneously has a unit of negative charge and an unpaired electron, as is known.

There is no distinct reduction peak on the CV of the obtained diethylphosphonate at room temperature and at -50 °C in the available range of potentials. Selectivity of ferrocene phosphorylation, high yield of monophosphorylation product and trace amounts of by-products in the optimal synthesis conditions indicate that the products are stable in electrolysis conditions and do not undergo further redox or chemical

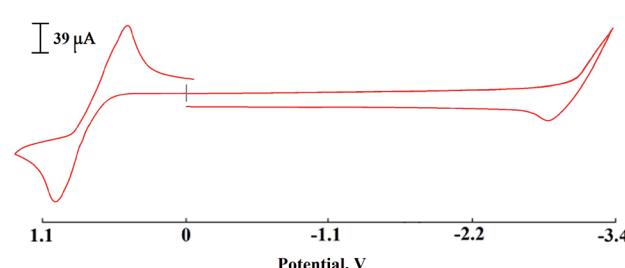


Fig. 3 Cyclic voltammetry of diethyl ferrocenyl phosphonate. Conditions: $T = -50$ °C, glassy carbon working electrode, Ag/AgCl ref. electrode, 0.5 mM [Fe], Bu_4NBF_4 background salt, DMF, 100 mV s^{-1} .

reactions (Table 1). We investigated the electrochemical behavior of diethyl ferrocenyl phosphonate in the electrolysis conditions (Fig. 3, Table 3). It has been found that the CV of this product differs strongly from CV of an unsubstituted ferrocene. So, diethyl ferrocenyl phosphonate is characterized by quasi-reversible oxidation peak at more positive potentials compared to that for ferrocene, $\Delta E_p^{a-c} = 0.44$ V (Table 3). Importantly, the phosphorylated ferrocene cathodic peak is not observed in the available potential range (Fig. 3). Apparently, heterogeneous rate constants of oxidation and reduction of the phosphorylated ferrocene is much less than those for ferrocene under similar conditions. The observed redox properties explain the success of the ferrocene phosphorylation.

ESR experiments

The key stage in the reaction under investigation is ferrocene reduction. Because up to now the conclusions about this process have been drawn only on the basis of voltammetry, we used modern research methods, namely, combined ESR – electrochemistry in order to clarify the key reduction product (and reagent in phosphorylation process). In the course of the ferrocene reduction in DMF at the temperature of -50 °C and the potential of -3.3 V, a signal was observed, the line width being equal to $\Delta H_{\text{peak-peak}} = 11$ Gs and $g = 2.000$ (Fig. 4). It is known that, in the ground state, the ferrocene Fc^0 is low-spin compound (D_{5h} symmetry, $3d^6$, $S = 0$).⁵³ It can be expected that, upon its reduction, a paramagnetic form $\text{Fc}^{\cdot-}$ should be formed, which has not previously been registered. However, the ESR spectra of radical anions of substituted ferrocenes were identified.^{54,55} Their g -factor values range from 2.003 to 2.028; the overall spectrum width varies from some units to tens of Gs;

Table 3 R-Ferrocene ($\text{R} = (\text{EtO})_2\text{P}(\text{O})^-$) electrochemical features. Conditions: -50 °C, glassy carbon working electrode, Ag/AgCl ref. electrode, 0.5 mM [R-Fc], Bu_4NBF_4 background salt, DMF, 100 mV s^{-1}

Oxidation, $\text{R-Fc}^0/\text{R-Fc}^+$			Reduction, $\text{R-Fc}^0/\text{R-Fc}^{\cdot-}$		
E_p^a/E_p^c , V	ΔE_p^{a-c} , V	$E_{1/2}$, V	E_p^c/E_p^a , V	ΔE_p^{c-a} , V	$E_{1/2}$, V
0.94/0.50	0.44	0.72	$-/-2.95$	—	—

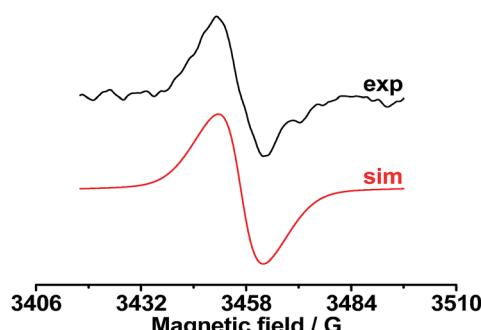


Fig. 4 ESR signal of reduced ferrocene (at -3.3 V) in a DMF solution, -50 °C. $g = 2.000$, $\Delta H_{\text{peak-peak}} = 11$ Gs.

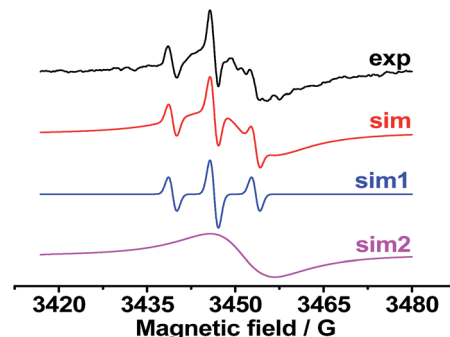


Fig. 5 ESR signals of reduced ferrocene at -3.9 V in a DMF solution at the temperature of -50 °C. sim1: $g = 2.0063$, 2: $a_H = 7$ Gs $\Delta H = 0.7$ Gs; sim2: $g = 2.002$, $\Delta H_{\text{peak-peak}} = 11$ Gs.

and the intensity of such spectra, as a rule, is not high. The low intensity can be caused by an inner-sphere reorganization of the ferrocene molecule, as assumed in the cited ref. 45 In this process, as well as in case of a neutral ferrocene, the spin state of the system probably changes. In all the substituted ferrocenes, the electron transfer to the Cp ligands occurs, and in some cases even splittings on hydrogen nuclei of one of the cyclopentadiene rings are registered.⁵⁶ Often, as in our case, only a relatively wide single line with no splitting is observed. The lifetime of the paramagnetic product amounts to 1 to 2 minutes in the DMF solution, according to time of the spectrum disappearance after the potential has been removed from the working electrode. This coincides with the data on the lifetime of the ferrocene anion obtained previously.⁴⁵ The foregoing makes it possible to suppose that the registered spectrum is attributable to the ferrocene radical anion. The g -factor value gives the evidence that, as in the case of substituted ferrocenes, the electron transfer occurs with participation of the orbital of the ligand but not iron.

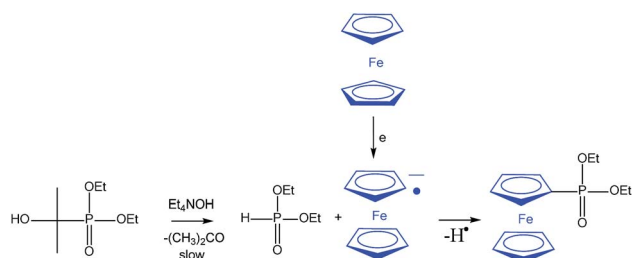
At further increasing negative potential of the electrode, the ESR spectra become more complicated (Fig. 5). It is most likely that they correspond to paramagnetic products of ferrocene molecule decomposition. The simulated signal sim1 with a splitting from two protons refers to a derivative of the free ligand without the ferrocene structure. The simulated signal sim2 most likely refers to a fragment with Fe. ESR signals exist for a long time after the potential has been disconnected, but their intensity did not reduce for at least half an hour at the temperature of -50 °C.

Reaction scheme

The following Scheme 2 can be proposed for the electrochemical synthesis of phosphorylated ferrocene:

In fact, in the reaction conditions we simultaneously generated dialkyl H -phosphonate from $(\text{Me})_2\text{C}(\text{OH})\text{P}(\text{O})(\text{OC}_2\text{H}_5)_2$ by a known reaction, as well as ferrocene radical anions, which react with each other, ultimately producing a phosphorylated ferrocene with good yield in a single stage. The proposed scheme is the best possible, but it does not preclude any other separate stage that might lead to the same final product.





Scheme 2 Electrochemical synthesis of ferrocene derivative.

Conclusions

Thus, the ferrocene radical anion ESR spectrum was recorded during Fc electrochemical reduction at the temperature of -50°C for the first time. We proposed new approach to the synthesis of phosphorylated ferrocene in one stage using α -hydroxyethylphosphonate and phosphorous acid as phosphorylating agents with the total yield up to 90%, and 36%, respectively.

Experimental

Cyclic voltammetry

The BASi Epsilon E2P (USA) electrochemical workstation was used for voltammetric measurements. The device comprises a measuring unit, a Dell Optiplex 320 computer with Epsilon-EC-USB-V200 software. As background electrolytes, tetrafluoroborate of tetrabutylammonium $(\text{C}_4\text{H}_8)_4\text{NBF}_4$ was used. The working electrode was a stationary disc glassy-carbon electrode (the surface area of 6 mm^2). Ag/AgCl (0.01 M) was used as a reference electrode, which was linked to the solution on the cell using a modified Luggin capillary filled with the background electrolyte (0.1 M Bu_4NBF_4 in DMF). Thus, the assembled electrode had two sections, each of which was completed with an ultra-thin frit glass (Vycor) to divide the AgCl from the analyzed compound.

A platinum wire was used as an auxiliary electrode. The curve recording was performed at the potential linear sweep rate of 100 mV s^{-1} . The measurements were performed in a temperature-controlled electrochemical cell (volume from 1 ml to 5 ml) in an inert gas atmosphere (N_2). The cooling of the researched solutions was performed with frozen carbon dioxide.

Between measurements or prior to the registration of a voltammetry wave, the solution was actively stirred with a magnetic stirrer in the atmosphere of constant inflow of an inert gas that was run through a dehydrating system, and then through a BI-GAScleaner (manufactured by OOO Modern Laboratory Equipment, Novosibirsk) nickel-based purification system to remove any trace quantity of oxygen.

ESR research

Liquid samples for the ESR spectra registration were freed from oxygen by applying a three-time repeat of the following cycle: freezing in liquid nitrogen, pumping and defrosting. After the

last cycle, the electrolysis cell was filled with gaseous helium. The operating electrode was a gold spiral. The experiments were performed in DMF at -50°C , the background electrolyte was 0.1 M Bu_4NBF_4 , and the sweep rate $E(t)$ amounted to 0.1 V s^{-1} . The measurements were performed with a suite of hardware and software assembled on the basis of the electrochemical analogue with a potentiostat and a PWR-3 programmer, an ELEXSYS E500 X-range ESR spectrometer, an E14-440 ADC and DAC module (L-Card Company), a computer and an original three-electrode spiral cell.⁵⁷ The ESR spectra were simulated with the WinSim 0.96 (NIEHS) software.

Preparative electrochemical syntheses

All reactions were obtained in a dry argon atmosphere. The preparative electrolysis was performed using a direct current source B5-49 in a three-electrode cell with 40 ml volume with a separation of the anode and cathode compartments. The potential value of the working electrode was recorded using a direct-current V7-27 voltmeter in relation to the Ag/AgCl (0.01 M, NaCl) reference electrode that had two sections separated with Vycor, the second of which contained a saturated solution of the background salt in DMF. The surface area of the working platinum (Pt) U-shaped electrode amounted to 48.00 cm^2 . A ceramic plate with the pore rate of 900 nm was used as a membrane. During the preparative synthesis, the electrolyte was continuously stirred using a magnetic stirrer with a continuous inflow of inert gas that was run through a purification system in order to remove any traces of oxygen and other gaseous impurities.

NMR spectra were recorded with a Bruker AVANCE-400 multi-nuclear spectrometer (400.1 MHz (^1H), 100.6 MHz (^{13}C) and 162.0 MHz (^{31}P)). Chemical shifts are given in parts per million relative to SiMe_4 (^1H , internal solvent) and 85% H_3PO_4 (^{31}P , external).

Reagents and research subjects

Dimethylformamide ("extra pure" by Acrosorganics), was purified by means of double fractionation distillation over melting potash. Diethyl(2-hydroxypropan-2-yl)phosphonate was obtained through the method described in the literature.⁵⁸

Et_4NBF_4 was obtained by mixing 30–35% water solution of tetraethylammonium hydroxide, Et_4NOH and HBF_4 acid to a neutral indicator reaction. In the course of the reaction, a white crystal precipitation is deposited, which is filtered and dehydrated. The obtained powder salts were recrystallized from ethyl ester and were dried for 2 to 3 days in a vacuum at 55°C .

Ferrocene (98%) and H_3PO_4 (extra pure, 98%, Acrosorganics) were used without preliminary purification.

Et_4NOH (20% aqueous solution, Acrosorganics) was subjected to a complete dehydration to a white solid on Schlenk's system prior to the beginning of the experiment.

General method of ferrocene phosphorylation

Condition 1 (Table 1, no. 1). The ferrocene (2.69×10^{-3} mol) and Et_4NOH (4.72×10^{-3} mol dehydrated immediately before the synthesis) in the DMF solvent (40 ml) were added to the



electrochemical cell. Diethyl-2-hydroxypropane-2-yl phosphonate was added drop-wise evenly throughout the time of the whole synthesis (2.69×10^{-3} mol) in order to obtain mono-phosphonate. The electrolysis was performed on the Pt electrode in the electrochemical cell with a separation of the anode and the cathode spaces at the temperature of -50 °C in a dry argon atmosphere at the potential of the working electrode of -3.3 V in the galvanostatic mode. The transferred electricity quantity amounted to $2F$ per mole of phosphonate. Upon completion of the electrolysis, the reaction mixture was washed with a saturated solution of ammonium chloride (50 ml for 3 times) and extracted with benzene (70 ml for 3 times). After separation, the organic layer was dried over magnesium sulfate and the solvent was concentrated. Subsequently, the residue was purified by running through a chromatographic column filled with silica gel (eluent: ethyl acetate–hexane).

Condition 2 (Table 1, no. 2). As with the condition 1, but diethyl-2-hydroxypropane-2-yl phosphonate, 5.38×10^{-3} mol was used instead 2.69×10^{-3} mol to obtain 1,1'-ferrocenylbis(diethylphosphonate).

Condition 3 (Table 1, no. 3). As with the condition 1, but $[\text{NaOH} + \text{Et}_4\text{NBF}_4]$, 4.72×10^{-3} mol was used instead Et_4NOH .

Condition 4 (Table 1, no. 4). As with the condition 1, but HP(O)(OEt)_2 , 2.69×10^{-3} mol was used instead diethyl-2-hydroxypropane-2-yl phosphonate. The Pb plate was used as the working electrode.

Condition 5 (Table 1, no. 5). As with the condition 1, but H_3PO_3 , 2.69×10^{-3} mol was used instead diethyl-2-hydroxypropane-2-yl phosphonate. The Pb plate was used as the working electrode.

Diethyl ferrocenyl phosphonate (1). ^1H NMR (CDCl_3 , δ ppm): 1.37 (t, 6H, $^3J_{\text{HH}} = 7.1$ Hz); 4.15–4.56 (m, 13H); ^{31}P NMR (CDCl_3 , δ ppm): 27.1; ^{13}C NMR (CDCl_3 , δ ppm): 16.9; 62.1; 67.3 (d, $^1J_{\text{CP}} = 215$ Hz); 70.3; 71.6; 71.92. IR (KBr, ν ; cm^{-1}): 2987, 2925, 2879 ($-\text{CH}_3$, $-\text{CH}_2-$), 1425 (P–C), 1248 (P=O), 1052 (P–O). EIMS, m/z : 322.15 [M^+]; anal. calc.: C, 52.20; H, 5.95; Fe, 17.34; O, 14.90; P, 9.62; for $\text{C}_{14}\text{H}_{19}\text{FePO}_3$; found: C, 52.14; H, 5.91; P, 9.58, Fe, 17.24. The spectroscopic data for diethyl ferrocenyl phosphonate matched that reported in the literature.²⁸

1,1'-Ferrocenylbis(diethylphosphonate) (2). ^1H NMR (CDCl_3 , δ ppm) 1.33 (t, 12H, $^3J_{\text{HH}} = 6.9$ Hz), 4.11–4.60 (m, 16H); ^{31}P NMR (CDCl_3 , δ ppm) 25.9; ^{13}C NMR (CDCl_3 , δ ppm) 16.9, 62.3, 68.8 (d, $^1J_{\text{CP}} = 214$ Hz), 73.4, 74.3, 74.3. IR (KBr, ν ; cm^{-1}): 2995, 2931, 2885 ($-\text{CH}_3$, $-\text{CH}_2-$), 1419 (P–C), 1245 (P=O), 1055 (P–O). EIMS, m/z : 458.57 [M^+]; anal. calc.: C, 47.18; H, 6.16; Fe, 12.19; O, 20.95; P, 13.52 for $\text{C}_{18}\text{H}_{28}\text{FeO}_6\text{P}_2$; found: C, 47.16; H, 6.09, P, 13.45, Fe, 12.13. The spectroscopic data for 1,1'-ferrocenylbis(diethylphosphonate) matched that reported in the literature.²⁸

Ferrocenylphosphonic acid (3). ^1H NMR (CD_3OD , δ ppm): 4.33 (s, 5H); 4.44–4.51 (m, 4H); ^{31}P NMR (CD_3OD , δ ppm): 24.6; ^{13}C NMR (CDCl_3 , δ ppm) 67.0, 71.1 (d, $^3J_{\text{CP}} = 11$ Hz), 72.4 (d, $^2J_{\text{CP}} = 13$ Hz), 74.5 (d, $^1J_{\text{CP}} = 165$ Hz), IR (KBr, ν ; cm^{-1}): 1196 (P=O), 1030 (P–O). EIMS, m/z : 266.70 [M^+]; anal. calc.: C, 45.11; H, 4.13; P, 11.65, Fe, 20.97. for $\text{C}_{10}\text{H}_{11}\text{FePO}_3$ found: C, 45.16; H, 4.10; P, 11.69, Fe, 20.60. The spectroscopic data for ferrocenylphosphonic acid matched that reported in the literature.²⁸

Acknowledgements

The work was supported with a grant from the Russian Science Foundation No. 14-23-00016.

Notes and references

- P. Barbaro, C. Bianchini, G. Giambastiani and S. L. Parisel, *Coord. Chem. Rev.*, 2004, **248**, 2131.
- T. J. Colacot, *Chem. Rev.*, 2003, **103**, 3101.
- A. Togni and T. Hayashi, *Ferrocenes: homogeneous catalysis, organic synthesis, material science*, Wiley-VCH, Weinheim, 1995.
- H. B. Kagan, P. Diter, A. Gref, D. Guillaneux, A. Masson-Szymczak, F. Rebière, O. Riant, O. Samuel and S. Taudien, *Pure Appl. Chem.*, 1996, **68**, 29.
- C. J. Richards and A. J. Locke, *Tetrahedron: Asymmetry*, 1998, **9**, 2377.
- R. C. J. Atkinson, V. C. Gibson and N. J. Long, *Chem. Soc. Rev.*, 2004, **33**, 313.
- P. Stepinicka, *Ferrocenes: ligands, materials and biomolecules*, Chichester, 2008.
- A. Togni, N. Bieler, U. Burckhardt, C. Köllner, G. Pioda, R. Schneider and A. Schnyder, *Pure Appl. Chem.*, 1999, **71**, 1531.
- L.-X. Dai, X.-L. Hou, W.-P. Deng, S.-L. You and Y.-G. Zhou, *Pure Appl. Chem.*, 1999, **71**, 1401.
- L.-X. Dai, T. Tu, S.-L. You, W.-P. Deng and X.-L. Hou, *Acc. Chem. Res.*, 2003, **36**, 659.
- T. J. Colacot, *Chem. Rev.*, 2003, **103**, 3101.
- X. L. Hou, S. L. You, T. Tu, W. P. Deng, X. W. Wu, M. Li, K. Yuan, T. Z. Zhang and L. X. Dai, *Top. Catal.*, 2005, **35**, 87.
- R. Gómez Arrayás, J. Adrio and J. C. Carretero, *Angew. Chem., Int. Ed.*, 2006, **45**, 7674.
- M. Ritte, C. Bruhn and U. Siemeling, *Z. Naturforsch., B: J. Chem. Sci.*, 2014, **69**, 906.
- M. Neel, A. Panossian, A. Voituriez and A. Marinetti, *J. Organomet. Chem.*, 2012, **716**, 187.
- D. Astruc, in *Organometallic Chemistry and Catalysis*, Springer-Verlag, Berlin, 2007.
- M. N. Khrizanforov, D. M. Arkhipova, R. P. Shekurov, T. P. Gerasimova, V. V. Ermolaev, D. R. Islamov, V. A. Miluykov, O. N. Kataeva, V. V. Khrizanforova, O. G. Sinyashin and Y. H. Budnikova, *J. Solid State Electrochem.*, 2015, **19**, 2883.
- D. Schaarschmidt and H. Lang, *Organometallics*, 2013, **32**, 5668.
- W.-Y. Wang, N.-N. Ma, L. Wang, C.-L. Zhu, X.-Y. Fang and Y.-Q. Qiu, *Dyes Pigm.*, 2016, **126**, 29.
- V. Mereacre, M. Schlageter, A. Eichhöfer, T. Bauer, J. A. Wolny, V. Schünemann and A. K. Powell, *J. Magn. Magn. Mater.*, 2016, **407**, 87.
- S. Takenaka, Y. Uto, H. Saita, M. Yokoyama, H. Kondo and W. D. Wilson, *Chem. Commun.*, 1998, 1111.
- S. Sato and S. Takenaka, *J. Organomet. Chem.*, 2008, **693**, 1177.

23 S. Watanabe, S. Sato, K. Ohtsuka and S. Takenaka, *Anal. Chem.*, 2011, **83**, 7290.

24 L. V. Snegur, A. A. Simenel, A. N. Rodionov and V. I. Boev, *Russ. Chem. Bull.*, 2014, **63**, 26.

25 L. V. Snegur, Y. S. Nekrasov, N. S. Sergeeva, Z. V. Zhilina, V. V. Gumenyuk, Z. A. Starikova, A. A. Simenel, N. B. Morozova, I. K. Sviridova and V. N. Babin, *Appl. Organomet. Chem.*, 2008, **22**, 139.

26 E. F. Jason and E. K. Fields, *J. Org. Chem.*, 1962, **27**, 1402.

27 G. P. Sollott and E. Howard, *J. Org. Chem.*, 1962, **27**, 4034.

28 G. R. Knox, P. L. Pauson and D. Willison, *Organometallics*, 1992, **11**, 2930.

29 O. Oms, J. Le Bideau, A. Vioux and D. Leclercq, *J. Organomet. Chem.*, 2005, **690**, 363.

30 M. Korb, D. Schaarschmidt and H. Lang, *Organometallics*, 2014, **33**, 2099.

31 S. R. Alley and W. Henderson, *J. Organomet. Chem.*, 2001, **216**, 637.

32 O. Oms, F. Maurel, F. Carré, J. Le Bideau, A. Vioux and D. Leclercq, *J. Organomet. Chem.*, 2004, **689**, 2654.

33 R. P. Shekurov, V. A. Miluykov, D. R. Islamov, D. B. Krivolapov, O. N. Kataeva, T. P. Gerasimova, S. A. Katsyuba, G. R. Nasibullina, V. V. Yanilkin and O. G. Sinyashin, *J. Organomet. Chem.*, 2014, **766**, 40.

34 Y. H. Budnikova and O. G. Sinyashin, *Russ. Chem. Rev.*, 2015, **84**, 917.

35 T. Gryaznova, Y. Dudkina, M. Khrizanforov, O. Sinyashin, O. Kataeva and Y. Budnikova, *J. Solid State Electrochem.*, 2015, **19**, 2665.

36 T. V. Gryaznova, Y. B. Dudkina, D. R. Islamov, O. N. Kataeva, O. G. Sinyashin, D. A. Vicic and Y. H. Budnikova, *J. Organomet. Chem.*, 2015, **785**, 68.

37 M. Khrizanforov, S. Strekalova, T. Gryaznova, V. Khrizanforova and Y. Budnikova, *Russ. Chem. Bull.*, 2015, **8**, 1926.

38 C. Li, T. Yano, N. Ishida and M. Murakami, *Angew. Chem.*, 2013, **125**, 9983.

39 D. W. Allen, D. E. Hibbs, M. B. Hursthouse and K. M. A. Malik, *J. Organomet. Chem.*, 1999, **572**, 259.

40 G. A. Stark, T. H. Riermeier and M. Beller, *Synth. Commun.*, 2000, **30**, 1703.

41 M. Hayashi, T. Matsuura, I. Tanaka, H. Ohta and Y. Watanabe, *Org. Lett.*, 2013, **15**, 628.

42 N. G. Tsierkezos, *J. Solution Chem.*, 2007, **36**, 289.

43 R. R. Gagné, C. A. Koval and G. C. Lisensky, *Inorg. Chem.*, 1980, **19**, 2854.

44 N. Ricke, S. N. Eustis and K. H. Bowen, *J. Mass Spectrom.*, 2014, **357**, 63.

45 N. Ito, T. Saji and S. Aoyagi, *J. Organomet. Chem.*, 1983, **247**, 301.

46 V. V. Strelets, *Coord. Chem. Rev.*, 1992, **114**, 1.

47 Y. Mugnier, C. Moise, J. Tirouflet and E. Laviron, *J. Organomet. Chem.*, 1980, **186**, 49.

48 A. J. Bard, E. Garcia, S. Kukbarenko and V. V. Strelets, *Inorg. Chem.*, 1993, **32**, 3528.

49 N. E. Murr and A. Chaloyard, *J. Organomet. Chem.*, 1980, **193**, 60.

50 Y. H. Budnikova, T. R. Novoselova and Y. M. Kargin, *Russ. J. Gen. Chem.*, 1992, **62**, 19621.

51 A. P. Tomilov, B. I. Martynov and N. A. Pavlova, *J. Electroanal. Chem.*, 2001, **507**, 46.

52 A. Alberti, M. Benaglia, B. F. Bonini, M. Fochi, D. Macciantelli, M. Marcaccio, F. Paolucci and S. Roffia, *J. Phys. Org. Chem.*, 2004, **17**, 1084.

53 T. P. Gryaznova, S. A. Katsyuba, V. A. Milyukov and O. G. Sinyashin, *J. Organomet. Chem.*, 2010, **695**, 2586.

54 C. Elschenbroich and M. Cais, *J. Organomet. Chem.*, 1969, **18**, 135.

55 G. Bigam, J. Hooz, S. Linke, R. E. D. McClung, M. W. Mosher and D. D. Tanner, *Can. J. Chem.*, 1972, **50**, 1825.

56 E. V. Tretyakov, S. E. Tolstikov, G. V. Romanenko, A. S. Bogomyakov, D. V. Stass, M. K. Kadirov, K. V. Holin, O. G. Sinyashin and V. I. Ovcharenko, *Polyhedron*, 2011, **30**, 3232.

57 M. K. Kadirov, E. V. Tret'yakov, Y. G. Budnikova, K. V. Kholin, M. I. Valitov, V. N. Vavilova, V. I. Ovcharenko, R. Z. Sagdeev and O. G. Sinyashin, *Russ. J. Phys. Chem. A*, 2009, **83**, 2163.

58 F. Texier-Boullet and M. Lequette, *Tetrahedron Lett.*, 1986, **27**, 3515.

